



Recent inorganic carbon increase in a temperate estuary driven by water quality improvement and enhanced by droughts

5 Louise C. V. Rewrie^{1*}, Burkard Baschek², Justus E. E. van Beusekom¹, Arne Körtzinger³,
Gregor Ollesch⁴, Yoana G. Voynova¹

1. Institute of Carbon Cycles, Helmholtz-Zentrum Hereon, 21502 Geesthacht, Germany.

2. Deutsches Meeresmuseum, 18439 Stralsund, Germany

3. GEOMAR, Helmholtz-Zentrum für Ozeanforschung Kiel, 24148 Kiel, Germany

10 4. Flussgebietsgemeinschaft Elbe (FGG Elbe), 39104 Magdeburg, Germany

Correspondence to: Louise C. V. Rewrie (louise.rewrie@hereon.de) and Yoana G. Voynova (yoana.voynova@hereon.de).

15 Abstract

Estuaries are an important contributor to the global carbon budget, facilitating carbon removal, transfer and transformation between land and coastal ocean. Estuaries are also susceptible to global climate change and anthropogenic perturbations. We find that a long-term significant
20 increase in dissolved inorganic carbon (DIC) of 6–21 $\mu\text{mol kg}^{-1} \text{yr}^{-1}$ (1997–2020) in a temperate estuary in Germany (Elbe Estuary), was driven by an increase in upper estuary particulate organic carbon (POC) content of 8–14 $\mu\text{mol kg}^{-1} \text{yr}^{-1}$. The temporal POC increase was due to an overall improvement in water quality observed in the form of high rates of primary production and a significant drop in biological oxygen demand. The magnitude of mid-estuary
25 DIC gain was equivalent to the increased POC production in the upper estuary, suggesting that POC is efficiently remineralized and retained as DIC in the mid-estuary, with the estuary acting as an efficient natural filter for POC. In the context of the significant DIC increase, the impact of a recent extensive drought period (2014–2020) significantly lowered the annual mean river discharge ($468 \pm 234 \text{ m}^3 \text{ s}^{-1}$) compared to the long-term mean ($690 \pm 441 \text{ m}^3 \text{ s}^{-1}$, 1960–2020).
30 During the drought period, the late spring internal DIC load in the estuary doubled. This suggests that the drought induced a longer dry season, starting in May (earlier than normal), increased the residence time in the estuary and allowed for a longer remineralization period for POC. Annually, 77–94 % of the total DIC export was laterally transported to coastal water, reaching $89 \pm 4.8 \text{ Gmol C yr}^{-1}$, and thus only a maximum of 23%, at $10 \text{ Gmol C yr}^{-1}$, was released via carbon dioxide (CO_2) evasion, between 1997 and 2020. Export of DIC to coastal
35 waters decreased significantly during the drought (2014–2020: $38 \pm 5.4 \text{ Gmol C yr}^{-1}$), on average by 24% compared to the non-drought period. In addition, we have identified that seasonal changes in DIC processing in an estuary require consideration in order to understand



40 both the long-term and future changes in air-water CO₂ flux, DIC export to coastal waters, as well as the impacts of prolonged droughts on the land-ocean carbonate system.

1. Introduction

45 Estuaries function as bioreactors in which biotic and abiotic processes act to augment, transform or attenuate carbon products (Bukaveckas, 2022). Despite successful initiatives to reduce eutrophication in estuaries and coastal waters, e.g. in the Wadden Sea (van Beusekom et al., 2019) and Delaware Estuary (Sharp, 2010), effects of anthropogenic eutrophication persist (Harding et al., 2019). Rivers still receive large nutrient concentrations sustaining phytoplankton growth, due to agricultural land use dominating the river catchments such as
50 along the Rhine and Elbe Rivers (Hardenbicker et al., 2016; Dähnke et al. 2022). Aquatic primary production supplies particulate organic carbon (POC) to and within estuaries, providing labile forms of carbon (Abril et al., 2002). This phytoplankton generated organic matter (OM) input into the estuary can lead to heterotrophic conditions in an estuary (Schöl et al. 2014), with OM further decomposed and converted into dissolved inorganic carbon (DIC).
55 Intense respiration of OM in estuaries can elevate the partial pressure of carbon dioxide ($p\text{CO}_2$) to above atmospheric levels, resulting in estuarine regions acting as a CO₂ sources to the atmosphere (Amann et al., 2015; Cai 2011). This reduces labile POC export to the adjacent coastal waters (Crump et al., 2017; Sanders et al., 2018). The rate of heterotrophic activity in estuaries, such as bacterial production and respiration, has been shown to correlate with
60 phytoplankton production (Hoch and Kirchman, 1993), POC concentration (Goosen et al., 1999) and temperature (Apple et al., 2006). This highlights the need to understand how changes in primary production of OM in the upstream estuary affect downstream heterotrophic conditions and production and export of DIC.

65 Over the last century, global temperatures have increased by 0.95 to 1.20°C (IPCC, 2022). Future global temperature increases are projected to intensify the hydrological cycle, while climate projections show that the frequency and length of droughts (Böhnisch et al., 2021), as well as the frequency and magnitude of heavy precipitation and flood events (Christensen and Christensen, 2003; Alfieri et al., 2015), will increase across Europe. Such modifications in the
70 hydrological balance will influence river systems, which are among the most sensitive ecosystems to climate change (Watts et al., 2015). While extreme floods tend to reduce residence time in estuaries and generate a large export of OM and nutrients from land to coastal



waters (Voynova et al., 2017), drought conditions can lengthen river and estuarine water residence time (Hitchcock and Mitrovic, 2015). This in turn can extend the retention of carbon and nutrients during droughts, permitting more extensive remineralization of organic material (Hitchcock and Mitrovic, 2015), and subsequently altering carbon and nutrient cycling. With hydrological droughts predicted to become more frequent and extensive in Europe (Forzieri et al., 2014; Williams et al., 2015), assessing how they influence carbon dynamics and estuarine biogeochemistry is essential for understanding and predicting carbon storage and export to the coastal region.

This study aims to highlight the functioning of an estuary under a multi-year drought, in the context of current regional climate change predictions. The Elbe Estuary is used as an example of a temperate estuary with a densely populated watershed, and subject to severe drought conditions between 2014 and 2020 (Barbosa et al., 2021; Moravec et al., 2021), with the period between 2014 and 2018 regarded as the worst multi-year soil moisture drought in Europe during the last 253 years (Moravec et al., 2021). To assess the impact on the estuarine ecosystem, we assess a longer period between 1997 and 2020. It has been described as the ecosystem recovery state of the estuary (Rewrie et al., in review), following major shifts in the ecosystem state after the 1980s heavy pollution. During the current recovery state, the annual mean DIC in the mid to lower Elbe Estuary has increased significantly by up to $11 \mu\text{mol L}^{-1} \text{yr}^{-1}$ from 1997 to 2018 (Rewrie et al., in review), but the source of this increase remains unclear. The current study has extended this time period by two years with further available data, and aims to (1) identify the reasons for the significant DIC increase, and (2) investigate how climate change has modulated this trend since the onset of the recent drought. Data for organic and inorganic carbon content supported by water quality measurements are used to assess the long-term changes in the carbonate system in the Elbe Estuary between 1997 and 2020, and with focus on the recent drought.

100 **2 Methods and Data**

2.1 Study site

The temperate Elbe Estuary is a well-mixed, mesotidal coastal plain estuary, with a maximum turbidity zone (MTZ) extending from around Elbe-km 650 to 700 (Fig.1a, Amann et al., 2015). The estuary stretches over 142 km from the tidal border at the Geesthacht Weir to the mouth of



the estuary at Cuxhaven, Germany. It connects one of the largest rivers in Northern Europe, the Elbe, to the German Bight in the southern North Sea. The Elbe Estuary was separated into seven zones designated by the TIDE project (Geerts et al., 2012). In this study, the zones are sub-
 110 grouped into five regions: the upper estuary (z1), Hamburg Harbour (z2–z3), middle (mid, z4–z5), lower (z6), and outer (z7) estuary.

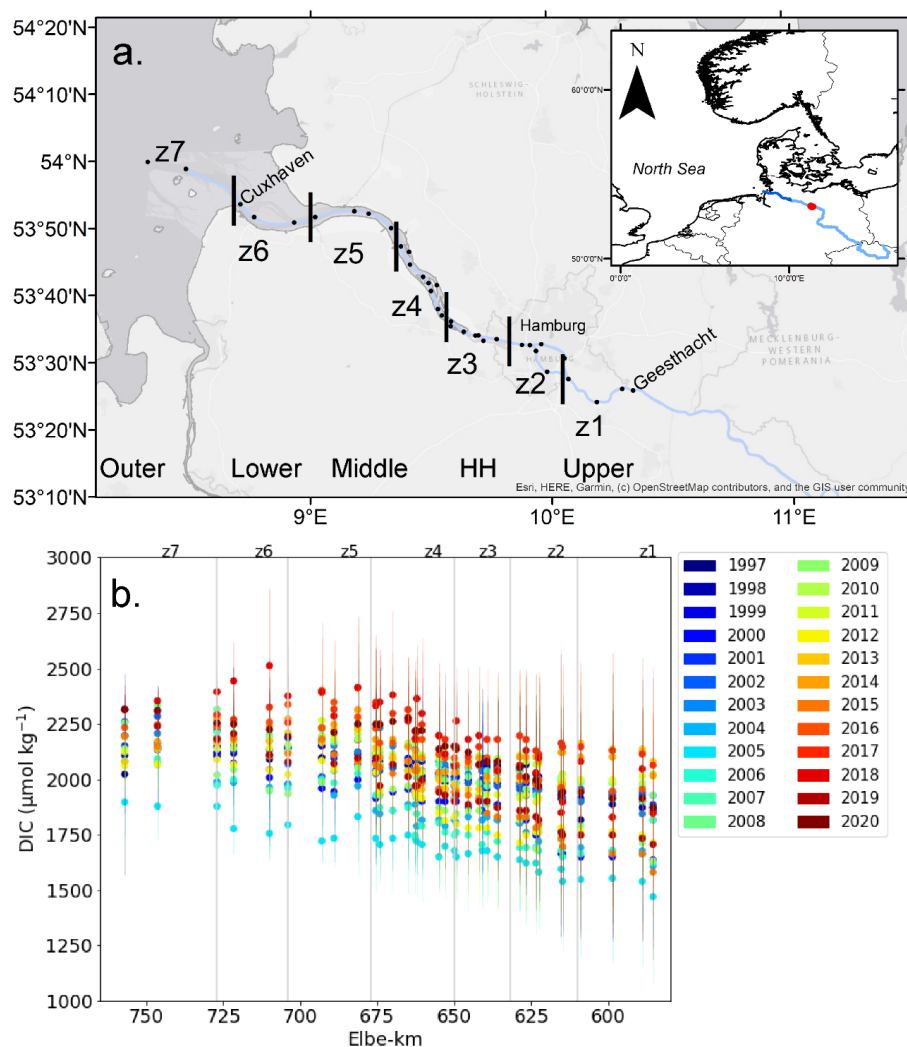


Figure 1: a) Map of the Elbe, separated into seven zones designated by the TIDE project (Geerts et al., 2012), with sub-groups: the upper estuary (z1), Hamburg Harbour (HH, z2–z3), middle (mid, z4–z5), lower (z6), and outer (z7) estuary. The black dots are the helicopter sampling stations with Geesthacht at 585.5 Elbe-km and Cuxhaven at 727 Elbe-km. The Elbe-km count
 115



is the distance from the Elbe passing the border between the Czech Republic and Germany. Insert map: The tidal estuary (dark blue), the non-tidal Elbe River (light blue) and the Neu Dauchau gauging station (536.4 Elbe-km, red) are indicated. b) Mean annual DIC in the Elbe Estuary from 1997–2020, with error bars representing the standard deviation from the mean.

2.2 Data sources

Data for DIC, POC and key ecosystem parameters (dissolved oxygen (DO), pH, biological oxygen demand (BOD₇)) were acquired from the data portal of the Flussgebietsgemeinschaft Elbe (FGG, River Basin Community; <https://www.fgg-elbe.de/elbe-datenportal.html>) for 1997 to 2020. The FGG Elbe took synoptic surface water samples from 36 stations in the estuary (Fig. 1a) by helicopter at full ebb current (ARGE Elbe, 2000). Sampling was generally carried out in February, May, June, July, August and November (see Rewrie et al. (in review) for a detailed description). The samples for DIC were analysed at FGG Elbe laboratories during the analysis of total dissolved carbon, in order to determine both DIC and dissolved organic carbon (DOC). Methods for organic carbon, DIC, dissolved oxygen (DO), pH and BOD₇ are listed in Table S1, and further described in Rewrie et al. (in review). The apparent oxygen utilization (AOU) was calculated (see Eq. S1) and is provided in the supplementary online materials (SOM).

2.3 River discharge

Daily freshwater discharge data (1960–2020) from Neu Darchau gauging station (536.4 Elbe-km, Fig. 1a) were also obtained from the FGG Elbe data portal (<https://www.elbe-datenportal.de/>). The historical mean river discharge (1960–2020) and the discharge during the drought period (2014–2020) were calculated, and the significance of the difference between the two periods (medians) was assessed using the Mann-Whitney-U-test, since both datasets presented a non-normal distribution from a Shapiro-Wilk test ($p < 0.05$). The significance of a monthly river discharge trend during the recovery state (1997–2020, Rewrie et al. (in review)) was assessed with the Pearson Correlation Coefficient.

2.4 Calculation for carbonate parameters (total alkalinity and pCO₂)

150



Using the CO2SYS program version 2.5 in Excel, the aquatic carbonate system parameters CO₂ partial pressure ($p\text{CO}_2$) and total alkalinity (TA) were calculated from measured DIC, temperature, salinity, pH and, when available, phosphate and silicate (Lewis and Wallace, 1998), applying the carbonic acid dissociation constants K_1 and K_2 of Cai and Wang (1998).
155 DIC concentrations were reported as whole, rounded numbers in mg L^{-1} , and for the carbonate system calculations, these were converted into $\mu\text{mol kg}^{-1}$. Rewrie et al. (in review) provide an extensive evaluation of the FGG Elbe DIC data, with an estimated analytical uncertainty of 99.7-102.5 $\mu\text{mol kg}^{-1}$ for DIC. The propagation of uncertainties for the calculated $p\text{CO}_2$ and TA (Orr et al., 2018) were determined using the estimated DIC analytical uncertainty, uncertainties
160 of the involved constants provided in Orr et al. (2018) and the recommended total standard uncertainty for pH of 0.01.

The median of the uncertainty output from the CO2SYS program for $p\text{CO}_2$ was 209 μatm (18% uncertainty relative to the mean $p\text{CO}_2$) and for TA was 100 $\mu\text{mol kg}^{-1}$ (5% uncertainty relative
165 to the mean TA) in the Elbe Estuary (z1–z7) between 1997 and 2020 (Table S2). Calculated TA and $p\text{CO}_2$ are comparable to previously published measured TA and calculated $p\text{CO}_2$ by Amann et al. (2015) between 2009 and 2011, with similar along-estuary patterns and magnitude. An example of the comparison for August 2010 is shown in Fig S1. Measured TA and calculated $p\text{CO}_2$ in June 2019 by Norbistrath et al. (2022) are also comparable to the
170 calculated TA and $p\text{CO}_2$ in this study (Table S3).

2.5 Statistical analyses for along-estuary carbonate parameters and upper estuary POC

For every zone, the Pearson Correlation Coefficient was applied to the winter (February),
175 autumn (November), late spring (May) and summer (June, July and August (JJA)) DIC, TA and $p\text{CO}_2$ to assess the trend and seasonal change from 1997 to 2020. The Pearson Correlation Coefficient was also applied to the late spring and summer POC in the upper region (z1) over time, when we assume that z1 represents the river input into the estuary. The difference in DIC concentration between the mid, lower and outer estuary (z4–z7) relative to the upper region
180 (ΔDIC) was used to determine the along-estuary DIC gain over time (1997–2020) in late spring and summer. The Pearson Correlation Coefficient was used to assess the dependency of along-estuary DIC gain (ΔDIC) on upper estuary POC concentration (z1).



185 2.6 Upper estuary POC loads as a driver of DIC loading

POC loads in the upper estuary (z1) and DIC loads in the estuary in Gmol C month^{-1} were calculated (Eqs. S2–S3). The differences in DIC load between the upper region (z1) and the mid to lower regions (z4–z6) were quantified to estimate the internal DIC load (Eqs. S4–S5).
190 A correction factor was applied to each estuarine zone (Amann et al., 2015) to account for tributary inputs along the estuary. The statistical differences between internal DIC loads during the recent drought (2014–2020) and non-drought (1997–2013) periods, and the differences between the internal DIC load in the mid-lower estuary and the POC load in the upper estuary (z1), for May to August were tested. The independent t-test was used for datasets that presented
195 a normal distribution from a Shapiro-Wilk test ($p < 0.05$), and the Mann-Whitney U Test was applied to the datasets that presented a non-normal distribution. The months of August 2002, August 2010 and June–July, 2013 were excluded from the statistical analysis as anomaly flood months (Kienzler et al., 2015, Voynova et al. 2017).

200 2.7 Air-water CO_2 exchange

The flux of CO_2 between water and atmosphere in $\text{mol m}^{-2} \text{d}^{-1}$ was estimated for each sampled station, in the upper to lower region (Fig. 1a), between 1997 and 2020 with the equation

$$F = k \times \alpha \times (p\text{CO}_{2(\text{water})} - p\text{CO}_{2(\text{atmosphere})}), (1)$$

205 with k as the gas transfer velocity, α as the solubility coefficient of CO_2 (calculated from Weiss 1974: in $\text{mol kg}^{-1} \text{atm}^{-1}$). $p\text{CO}_{2(\text{water})}$ was calculated from the FGG Elbe DIC and pH samples, and $p\text{CO}_{2(\text{atmosphere})}$, according to Dickson et al. (2007) with

$$p\text{CO}_{2(\text{atmosphere})} = X\text{CO}_{2(\text{atm})} \times (P_{\text{ATM}} - p\text{H}_2\text{O}), (2)$$

with the molar fraction of CO_2 in dry air $X\text{CO}_2$ obtained from Global Monitoring Laboratory
210 (Lan et al., 2023). Daily mean ambient air pressure (P_{ATM}) from E-OBS meteorological data for Europe (Cornes et al., 2018) from the Copernicus Climate Data Store (<https://cds.climate.copernicus.eu>) was selected for the Elbe Estuary region and each sampling station (Fig. 1). The saturated water partial pressure $p\text{H}_2\text{O}$ in atm was derived according to Weiss and Price (1980) with

$$215 \quad \ln p\text{H}_2\text{O} = 24.4543 - 67.4509 \left(\frac{100}{T}\right) - 4.8489 \ln\left(\frac{T}{100}\right) - 0.000544 \text{ Sal}, (3)$$



where T denotes in-situ temperature in Kelvin and Sal is the salinity of the sample. The gas transfer velocity k was calculated after Wanninkhof (2014) as follows

$$k = 0.251 \times (U_{10})^2 \times \left(\frac{Sc}{600}\right)^{-0.5}, (4)$$

where 0.251 is the coefficient of gas transfer, U_{10} is the wind speed in m s^{-1} measured *in situ* at 10 m height from E-OBS meteorological data for Europe (Cornes et al., 2018 from <https://cds.climate.copernicus.eu>). The Schmidt number (Sc) for CO_2 in freshwater was calculated according to Wanninkhof (2014) as a function of water temperature. The uncertainty estimate of k has been estimated to 20 % (Wanninkhof, 2014). We find a good fit of air-water CO_2 flux estimates to those calculated in Norbistrath et al. (2022) shown in Table S4. The tentative annual air-water CO_2 flux, with the total area of the Elbe Estuary of 276.6 km^2 between Geesthacht and Cuxhaven, Germany, derived via GIS by Amann et al. (2015), were used to estimate the air-water CO_2 flux in Gmol C yr^{-1} .

3 Results

Two main features are notable in the mean annual DIC concentration: (1) DIC increased from the upper freshwater estuary towards the mid to lower estuary (Fig. 1b), suggesting along-estuary accumulation of DIC, with a maximum in the MTZ and lower estuary ($z5$ – $z6$); (2) a pronounced DIC increase over time, reaching a maximum mean annual DIC in the lower estuary ($z6$, $2512 \pm 349 \mu\text{mol kg}^{-1}$) in 2018, which was 20% higher than in 1997 ($2090 \pm 364 \mu\text{mol kg}^{-1}$). This is a distinctive feature of the along-estuary DIC pattern for the recovery ecosystem state (Rewrie et al. in review).

3.1 Drivers of DIC dynamics along the estuary and DIC increase in the Elbe Estuary

Since 1997, the lowest DIC in the upper region in late spring and summer coincided with high pH (9.4) and large negative AOU ($-288 \mu\text{mol L}^{-1}$), i.e. supersaturation with respect to atmospheric equilibrium. This suggests that dominating autotrophy depletes DIC in the upper estuary, and most likely the upstream river regions. The exception was between 2018 and 2020, when pH decreased to 7.7, and AOU had predominately positive values (Fig. 2d), up to $+117 \mu\text{mol L}^{-1}$, indicating a possible shift to dominating heterotrophy in $z1$, 4–6 years after the onset of the drought in 2014 (Fig. 2a).



The different estuarine regions (Fig. 1a) are clearly distinguishable in pH (Fig. 2c) and AOU (Fig. 2d). Between the Hamburg Harbour and the lower estuary in late spring to summer, pH decreased compared to the upper region, and AOU was positive, coupled with an along-estuary increase in DIC. This suggests dominating heterotrophic activity in the warmer months (see also Amann et al., 2015; Rewrie et al., in review) and accumulation of DIC in surface waters. In the outer estuary, pH increased and AOU was predominately negative, indicating dominating autotrophy in the coastal regions adjacent to the estuary. Changes in the along-estuary DIC concentrations over time (1997–2020) appear to be decoupled from the pH and AOU dynamics (Fig. 2b–d). When spring and summer DIC concentrations were lowest in 2005–2006, ranging between 914 $\mu\text{mol kg}^{-1}$ and 2040 $\mu\text{mol kg}^{-1}$, this minimum was not reflected in concurrent change in AOU or pH.

Significant POC increases occurred in late spring (May, 14 $\mu\text{mol C kg}^{-1} \text{ yr}^{-1}$) and summer (June–August, 8 $\mu\text{mol C kg}^{-1} \text{ yr}^{-1}$) in the upper estuary (Fig. 3, Table 1). A concurrent significant decrease of BOD₇ in late spring and summer (Fig. S2), suggests an improvement in water quality. This indicates a long-term intensification in production of OM in the upper estuary (z1) and in the river upstream of this region. Four years after the onset of the drought, POC dropped by 35% in summer 2018–2020 ($325 \pm 141 \mu\text{mol kg}^{-1}$), and this lower POC coincided with the shift to lower pH (Fig. 2c), and predominately positive AOU (Fig. 2d).

Coincident with the 1997–2020 POC increase in the upper estuary, DIC and TA increased significantly in the mid to outer estuary by up to 21 $\mu\text{mol kg}^{-1}$ in late spring (May) and 12 $\mu\text{mol kg}^{-1}$ in summer (June–August), with a significant positive correlation between mid-estuary DIC gain and upper estuary POC content in late spring. Also, in late spring, compared to the rest of the estuary, DIC concentration peaked in the mid-estuary (z5, 1997–2019) in 73% of the recent 10 years (2009–2019). In both late spring and summer, the DIC gain in the mid-estuary (286 ± 247 to $359 \pm 155 \mu\text{mol kg}^{-1}$) was not significantly different from the upper estuary POC (347 ± 94 to $377 \pm 165 \mu\text{mol kg}^{-1}$, Table S5 & S6). Thus, the amount of upstream POC (z1) available for remineralization was sufficient to account for the production of mid-estuary DIC. The mid-estuary was characterized by a TA to DIC ratio of < 1.0 (z4, Fig. 3), with the highest $p\text{CO}_2$ content, exceeding $> 1000 \mu\text{atm}$ in late spring and summer, indicating that the additional DIC input was in the form of $p\text{CO}_2$.

280



During summer, in 73% of all years, the along-estuary DIC was highest in the outer estuary between 1997 and 2020. This differs from the mid-estuary DIC peak in late spring (May) and suggests production in, or lateral transport of DIC into the outer estuary in summer. Mean summer AOU in the outer estuary was negative in 61% of all years (1997–2020). During these 285 years, the mean DIC was significantly and positively correlated with mean AOU ($r = 0.58$, $p < 0.05$) and negatively correlated with mean pH ($r = -0.58$, $p < 0.05$). These correlations demonstrate the control of primary production on DIC in the outer estuary during summer. When AOU was > 0 , there was no trend in DIC with AOU and pH. Along the estuary, the TA to DIC ratio increased to > 1.0 (Fig. 3), while $p\text{CO}_2$ decreased to a range of $65 \pm 58 \mu\text{atm}$ to 290 $821 \pm 363 \mu\text{atm}$, in the outer estuary, suggesting drawdown of DIC in this region.

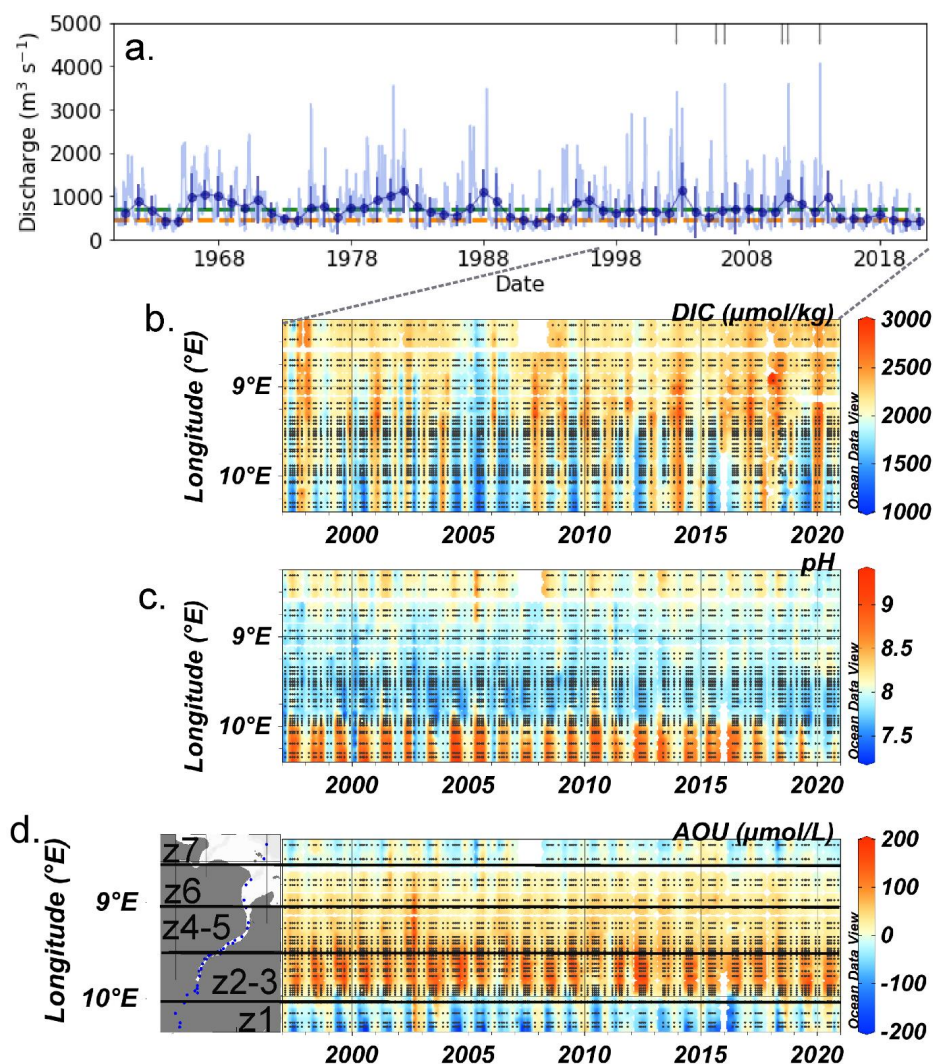


Figure 2. a) Daily Elbe River discharge (light blue), mean annual river discharge with error bars representing the standard deviation of the mean (dark blue) and flood events (grey marks) between 1960 and 2020. Long-term (1960–2020) mean annual Elbe River discharge of $690 \pm 441 \text{ m}^3 \text{ s}^{-1}$ (green dashed line) and the drought period (2014–2020) mean annual Elbe River discharge of $468 \pm 234 \text{ m}^3 \text{ s}^{-1}$ (orange dashed line). Hovmöller diagram of (b) DIC ($\mu\text{mol kg}^{-1}$), (c) pH and (d) apparent oxygen utilization (AOU in $\mu\text{mol L}^{-1}$), with map of sampling stations (also refer to Fig. 1a) and black lines separating the upper (z1), Hamburg Harbour (z2–z3), mid (z4–z5), lower (z6), and outer (z7) regions, in the Elbe Estuary from 1997–2020 (note different time-scale to the river discharge). The Hovmöller diagrams were produced with DIVA gridding in Ocean Data View and black dots represent the sampling stations.

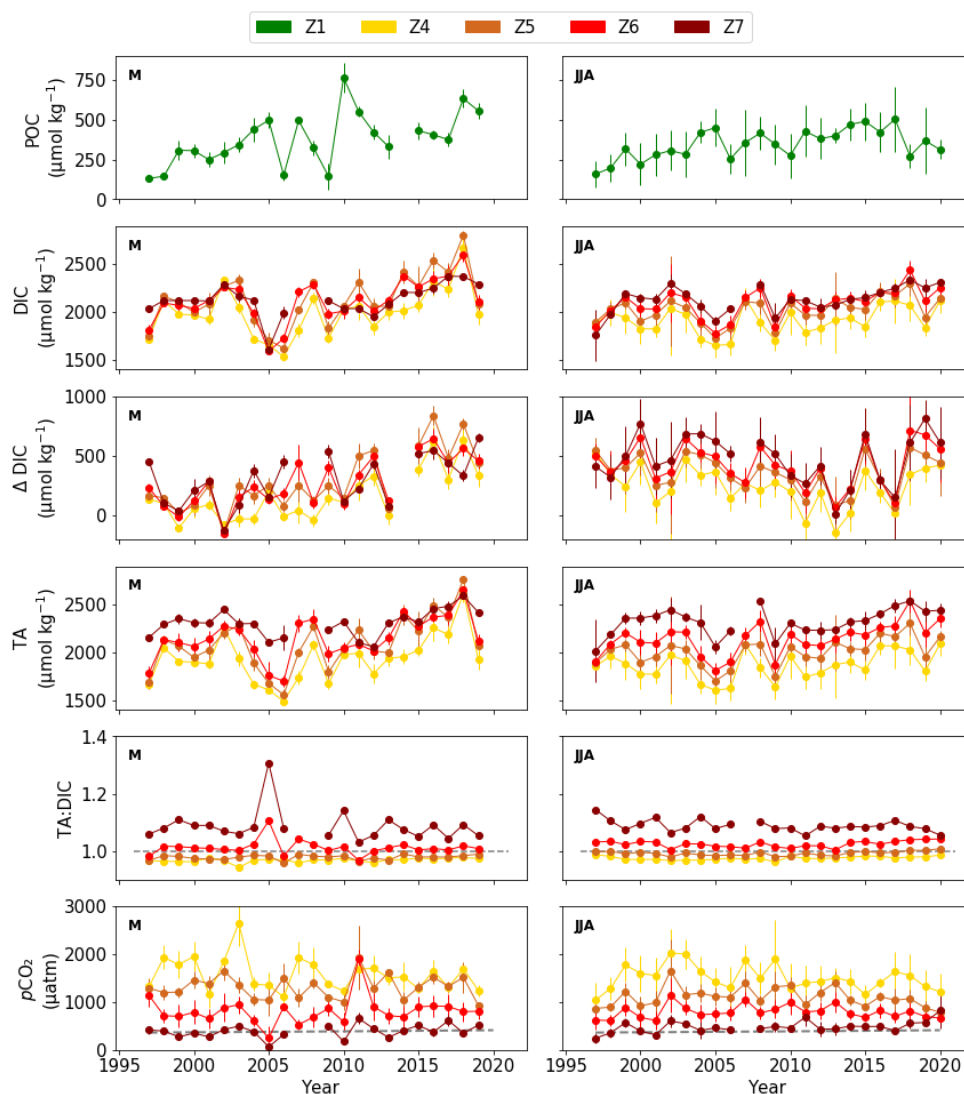


Figure 3. Late spring (May, M) and summer (June–August, JJA) POC in zone 1 (Z1) and DIC, along-estuary DIC gain (Δ DIC), TA, TA:DIC ratio (1 indicated by grey dashed line), and $p\text{CO}_2$, with atmospheric CO_2 values (grey dashed line) from Global Monitoring Laboratory (Lan et al., 2023), in the mid to outer estuary (zone (Z) 4–7, in Fig. 1b) from 1997 to 2020 (in May to 2019). Note differences in y-axis scales. Error bars represent the standard deviations of the mean.

310



Table 1. Pearson Correlation Coefficient (r) of late spring (May) and summer (June–August (JJA)) POC concentration in zone 1 ([C]) and DIC concentration ([C]), the along-estuary DIC gain (Δ DIC) and TA concentration in zones 4–7 in the Elbe Estuary with time (decimal year).

315 Highlighted are two levels of significance: $p < 0.05$ (red) and $p < 0.10$ (purple). The rate of change is given for POC, DIC and TA (β , $\mu\text{mol kg}^{-1} \text{yr}^{-1}$). Pearson Correlation Coefficient was also given between the along-estuary DIC gain (Δ DIC) with POC concentration in zone 1 (z_1). The Shapiro-Wilk test of normality was applied prior to statistical analysis. The Spearman Rank Correlation was applied to DIC in zone 7, Δ DIC in zone 4 and Δ DIC in zone 4 with POC concentration in zone 1 for May.

	Month	Zone	[C] vs time (1997–2020)*		Δ DIC vs time (1997–2020)*	Δ DIC Vs POC (z_1)*	[TA] vs time (1997–2020)*	
			r	β ($\mu\text{mol kg}^{-1} \text{yr}^{-1}$)			r	β ($\mu\text{mol kg}^{-1} \text{yr}^{-1}$)
POC	May	1	0.58	14				
	JJA	1	0.57	8				
DIC, Δ DIC or TA	May	4	0.40	15	0.67	0.44	0.42	16
		5	0.51	21	0.73	0.43	0.52	21
		6	0.50	17	0.71	0.30	0.49	16
		7	0.44	9	0.53	0.00	0.37	7
	JJA	4	0.29	6	-0.26	-0.47	0.31	7
		5	0.42	8	-0.19	-0.39	0.44	9
		6	0.50	11	-0.06	-0.30	0.51	12
		7	0.50	10	-0.10	-0.19	0.42	8

* Data for May from 1997–2019.

3.2 Influence of drought on estuarine DIC

325 From 2014 to 2020, mean annual Elbe River discharge of $468 \pm 234 \text{ m}^3 \text{ s}^{-1}$ was 32% lower than the long-term 1960–2020 mean at $690 \pm 441 \text{ m}^3 \text{ s}^{-1}$ (Fig. 2a, Table S8). This indicates that an inter-annual hydrological drought took place since 2014, characterized by overall reduced streamflow (Zink et al., 2016). Between 1997 and 2020, May was the only month with a significant negative trend in mean monthly river discharge ($r = -0.43$, $p < 0.05$), reaching lowest discharge of $264 \pm 19 \text{ m}^3 \text{ s}^{-1}$ in May 2020. Such low monthly discharge is usually observed during dry summer and early autumn months, with more extreme values in 2018–2019 at $< 200 \text{ m}^3 \text{ s}^{-1}$. This suggests that the drought extended the low discharge summer period into late spring, and most likely increasing the water residence time in the estuary, as seen by Bergemann et al. (1996).

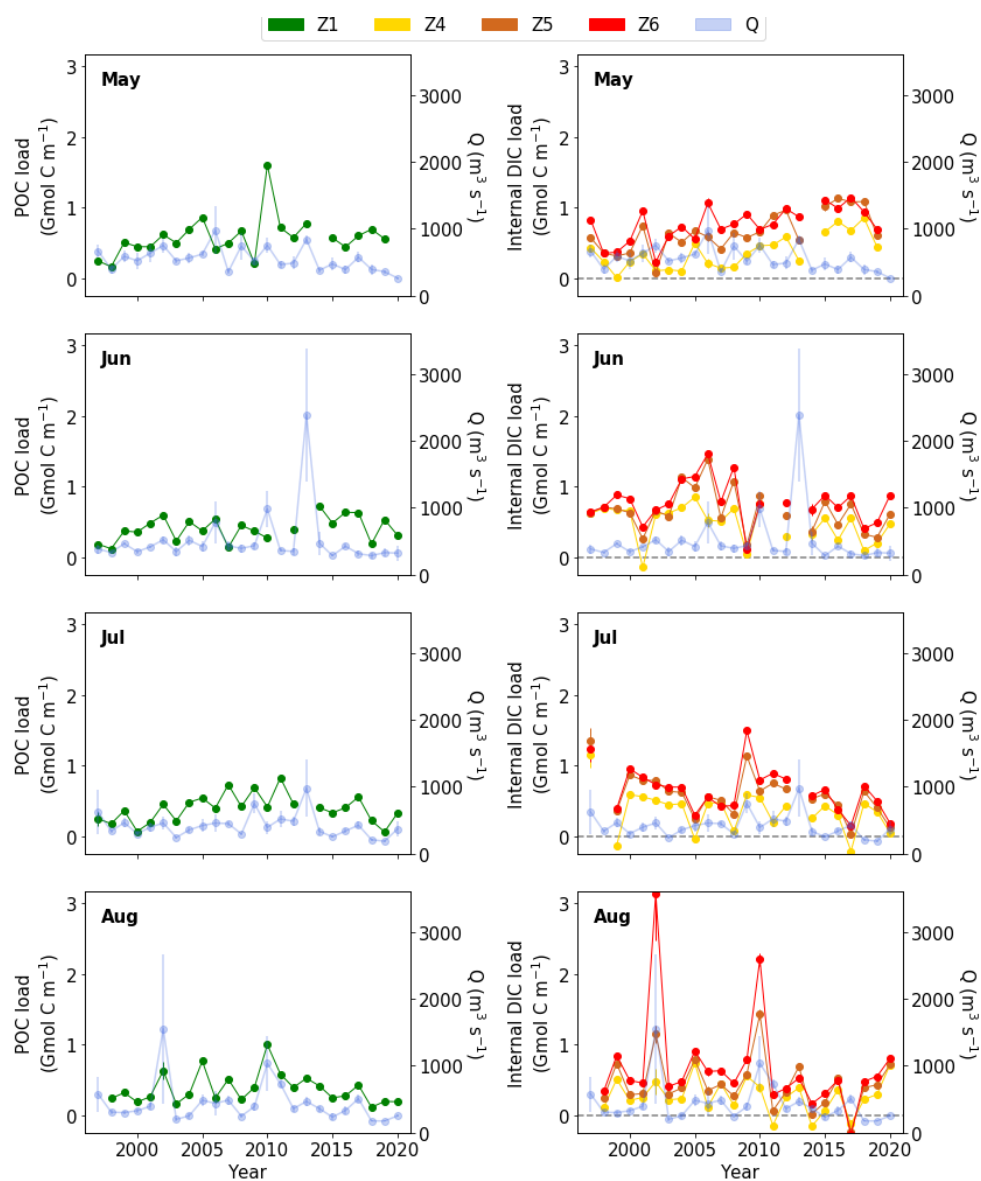
335



340 Despite this significant decrease in river discharge, in May, the internal DIC load in the mid to lower estuary was significantly higher during the drought period of 2014 to 2020, at 0.9 ± 0.22 Gmol C month⁻¹, compared to the non-drought period of 1997 to 2013 at 0.5 ± 0.27 Gmol C month⁻¹ (see Fig. 4 and Table S9–S10). In summer, the internal DIC load decreased significantly, by 35–42%, during the recent drought years (2014–2020), down to 0.3 ± 0.18 Gmol C month⁻¹ (June z4 and July z5–z6, Table S9–S10), compared to the non-drought period, ranging between 0.5 ± 0.27 and 0.7 ± 0.32 Gmol C month⁻¹ (1997–2013). The positive AOU and lower pH in 2018–2020 (Fig. 2c–d), suggest there was a shift from net autotrophy to net heterotrophy in the river, potentially leading to DIC production and larger input in the upper estuary. This would explain the elevated DIC concentrations in July–August 2017 for example (Fig. S3). Such dominating heterotrophy in recent years (2018–2020) and DIC generation in the upper region (z1), would subsequently reduce the internal DIC load in the mid to lower estuary (Fig. 4).

350 Overall, from May to August, the mid to lower estuary internal DIC load (z4–z6, Table S9–S10) during the drought (0.5 ± 0.33 Gmol C month⁻¹) was not significantly different from the non-drought period (0.6 ± 0.31 Gmol C month⁻¹). Therefore, during the drought, the May increase in internal DIC load was countered by an observed decrease in summer, ultimately resulting in no net change in the internal DIC load compared to the non-drought period (1997–355 2013). Albeit, the significant decrease in annual mean river discharge during the drought does significantly impact seasonal DIC production. Therefore in estuaries such as the Elbe Estuary, it is imperative to consider seasonality in carbon budget calculations.

In late spring (May) and summer (June–August), the mean POC load (0.3 ± 0.16 to 0.6 ± 0.29 360 Gmol C month⁻¹) in the upper estuary had the same magnitude as the internal DIC load (0.3 ± 0.25 to 0.7 ± 0.28 Gmol C month⁻¹) in the mid-estuary (1997–2020, Table S12), with no significant difference (z5 in May and z4 in June–August, Table S13). In contrast, the internal DIC load (0.5 ± 0.26 to 0.8 ± 0.30 Gmol C month⁻¹) in the lower estuary was significantly (1.3–1.9 times) greater than the upper estuary POC load (Table S12–S13). This means that while 365 POC from the upstream regions can account for the DIC production in the mid-estuary, in the lower estuary, an additional source of OM likely contributes to the DIC production therein.



370 Figure 4. Carbon load as POC in zone 1 (Z1) and the internal DIC load in the mid-lower estuary
 (zone (Z) 4-6), with zero internal DIC load (dashed grey line) and the respective monthly mean
 river discharge (Q) for each year (light blue). Error bars represent the standard deviations of the
 mean.

375



3.3 Annual inorganic carbon export estimates

The annual inorganic carbon export to the atmosphere and adjacent coastal waters was estimated to tentatively evaluate the overall inorganic carbon export dynamics in the Elbe Estuary between 1997 and 2020. The annual water-to-air CO₂ flux ranged between 4 and 10 Gmol C yr⁻¹, with an average flux of 6 ± 1.6 Gmol C yr⁻¹ and the highest flux recorded in 2020 (Fig. 5). The DIC export to adjacent coastal waters, based on the annual lower estuary DIC load (Eqs. S2–S3), ranged from 32 ± 0.9 to 89 ± 4.8 Gmol C yr⁻¹.

During the drought period (2014–2020), the DIC export to coastal waters (38 ± 5.4 Gmol C yr⁻¹) was significantly lower, by on average 24–31%, compared to the non-drought period (50 ± 6.4 Gmol C yr⁻¹ (excl. flood years) and 55 ± 14.0 Gmol C yr⁻¹ (incl. flood years), Table S15). In contrast, the annual water-to-air CO₂ flux was not significantly different during the drought (6 ± 1.9 Gmol C yr⁻¹) and non-drought period (6 ± 1.6 Gmol C yr⁻¹ (excl. flood years) and 6 ± 1.5 Gmol C yr⁻¹ (incl. flood years)).

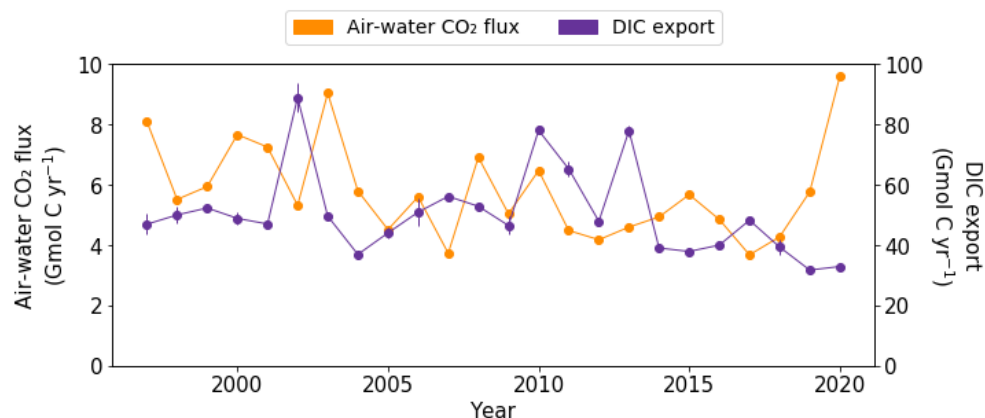


Fig. 5 Annual mean air-water CO₂ flux estimates in the Elbe Estuary and the annual mean DIC export, based on the lower estuary DIC load (Eqs. S2–S3), in Elbe Estuary. Note differences in y-axis scales. Error bars represent the standard deviations of the mean.

4 Discussion

Since 1997, the upper estuary and upstream regions have experienced a significant increase in POC in late spring and summer. Coupled with elevated pH reaching 9.4 and negative AOU,



this is evidence that dominating autotrophy in these upstream regions has become a larger source of labile POC to the mid–lower estuary between 1997 and 2020. Kamjunke et al. (2021) also reported high POC ($> 749 \mu\text{mol L}^{-1}$) in the lower Elbe River during summer 2018, with a strong correlation between POC and chlorophyll-a (chl-a), indicating a dominant contribution of phytoplankton to POC upstream of the Elbe Estuary. We suggest that the underlying reason for this significant increase in phytoplankton production is due to the amelioration of water quality in the river and upper estuary (IKSE 2010; Langhammer 2010; IKSE 2018), indicated by a BOD_7 decrease by more than half in summer (1997–2020, Fig. S2), opposite of the observed POC increase. This is evidence that the ecosystem state of the Elbe Estuary, and perhaps the Elbe River, is still changing during the recovery state, as suggested by Rewrie et al. (in review), following the major anthropogenic influences and social changes before and during the 1980s–1990s. Therefore, changes in water quality should be taken into account in regional and global estimates for carbon processing in estuaries. We also found that the along-estuary DIC pattern was driven by the DIC source concentrations in the upper estuary, likely due to a DIC drawdown by primary producers in the upstream regions of the Elbe River (e.g. in 2005–2006 Fig. 2). This highlights the influence of the upper regions as a source of carbon labile to the estuary, and the importance to evaluate the carbon dynamics from the watershed as well.

420

In late spring, the significant correlation between mid-estuary DIC gain and upper estuary POC (Table 1) suggests that the increase in OM in the upper estuary and upstream waters is driving the long-term DIC increase in the mid-estuary identified by Rewrie et al. (in review). Since the upper estuary POC in late spring and summer tripled since the onset of the recovery state in 1997, and POC mineralisation efficiency is a linear function of POC concentration (Abril et al., 2002), we expect a higher turnover of POC in the estuary in recent years. Subsequently this increases DIC production over time, as was observed in this estuary.

430

The magnitude of along-estuary DIC gain in the mid-estuary and POC input into the estuary show no significant difference in late spring and summer (Table S5). There are also no other major sources of carbon along the estuary (Abril et al., 2002), suggesting that POC was efficiently remineralized and converted to DIC by the mid-estuary. This is supported by Abril et al. (2002) who reported mineralisation of labile riverine POC simultaneously with an increase in SPM at the entrance of the MTZ (here z4). We find that POC drops to $< 4\%$ of SPM in May to August (1997–2020) in the mid estuary (z4–z5, Fig. S5), indicating widespread OM

435



rem mineralization in the estuary. This suggests that improving water quality in an ecosystem, following significant ecosystem state changes (Rewrie et al., in review), can result in an increase or decrease of the estuary's efficiency as a natural filter.

440 Most likely, a large part of POC from the Elbe is mineralized in the Hamburg Harbour (z2–z3),
in the oxygen minimum zone, as suggested by Amann et al. (2012), characterized by persistent
low pH and positive AOU (Fig. 2c–d). A low carbon to nitrogen ratio of suspended matter, with
high dissolved silicate concentration, found by Dähnke et al. (2022) corroborates this, most
likely with the dissolved silica values coming from diatom frustules. As a result of the POC
445 remineralization, $p\text{CO}_2$ increases exponentially from the Hamburg Harbour (e.g. Fig S1), and
reaches highest $p\text{CO}_2$ in the mid-estuary (z4), between 2.9 and 7.1 times that of the global mean
annual atmospheric CO_2 (Fig. 3). Similar $p\text{CO}_2$ ranges were previously calculated in the Elbe
Estuary (Amann et al., 2015; Norbistrath et al., 2022), and the calculated $p\text{CO}_2$ values match
data from August 2010 (Fig S1) and June 2019 (Table S3). We postulate that POC from the
450 upper estuary is therefore efficiently remineralized in the Hamburg Harbour, and is converted
into DIC as CO_2 , in the low pH regions (z2–z3, Fig. 2) and mid-estuary (z4–z5), also shown by
Amann et al. (2015). As along-estuary pH increases in the mid to the lower estuary (Fig. 2c),
accompanied by an along-estuary decrease in $p\text{CO}_2$ (Fig. 3), a speciation shift from $p\text{CO}_2$ to
bicarbonate (HCO_3^-) occurs, retaining CO_2 in the carbonate system buffer. Previous studies
455 (Kempe, 1982; Brasse et al., 2002) reported that seawater enriched in carbonate (CO_3^{2-}) buffers
by titration the freshwater high in $p\text{CO}_2$ and undersaturated with respect to calcite, in the low-
salinity (< 15 psu) mid to lower regions, thus preventing CO_2 flux to the atmosphere. TA
generation via calcium carbonate dissolution as described by Norbistrath et al. (2022) within the
Elbe Estuary can also convert the CO_2 to HCO_3^- . This could explain the observed continual
460 along-estuary gain of DIC. Internal remineralization of POC via respiration in the Elbe Estuary,
especially by the mid-estuary, and the equivalent POC concentration and along-estuary DIC
gain, indicate retention of carbon in the Elbe Estuary, rather than a significant loss to the
atmosphere. The mid and lower estuary concurrent increase in TA over time (Table 1 and Fig.
3), and absence of temporal $p\text{CO}_2$ increase (Fig. 3), indicates the produced DIC in the form of
465 $p\text{CO}_2$ was consistently converted to HCO_3^- . These findings emphasize the importance of the
estuary in the carbon processing along the land-to-ocean continuum.

Increasing alkalinity trend during the past century has been observed in river and estuarine systems (Raymond et al., 2008; Kaushal et al. 2013). However, we propose the temporal late



470 spring and summer DIC increase in the Elbe Estuary was not fuelled by internal production of
TA nor external inputs of TA via the Elbe River. Norbistrath et al. (2022) revealed calcium
carbonate dissolution as the main biogeochemical process producing TA in the Elbe Estuary,
which increases TA and DIC at a 2:1 ratio (Guo et al., 2008), and would therefore result in an
475 overall higher TA concentration compared to DIC. The higher DIC content compared to TA in
the mid-estuary (Fig. 3) confirms the along-estuary increase in DIC late spring and summer was
not fuelled by a change in CaCO_3 dissolution processes. The rise of TA in rivers can increase
TA in coastal ecosystems, as shown by a nearly 50% increase in TA export from the Mississippi
River to the Gulf of Mexico (Raymond et al., 2008), which was found to be anthropogenically
480 driven via cropland expansion, coupled with increased precipitation in the river catchment. In
the present study, the absence of temporal late spring and summer TA increase in the upper and
Hamburg Harbour regions (z1–z3, not shown) suggests the increase in carbonate parameters
(TA and DIC) was not driven by external river inputs into the estuary.

4.1 The recent drought modulates estuarine carbon cycling

485 The recent drought period (2014–2020) has altered estuarine carbon cycling in several ways.
Late spring (May) river discharge significantly decreased. By 2020, it reached levels (264 ± 19
 $\text{m}^3 \text{s}^{-1}$) usually observed during summer and early autumn, thus extending the dry summer
season into late spring. As a result, the estuarine water residence time increased compared to
490 non-drought years by approximately 3 times (Table S16), using a function estimated by
Bergemann et al. (1996), where a decrease from $700 \text{ m}^3 \text{ s}^{-1}$ to $250 \text{ m}^3 \text{ s}^{-1}$ would extend the
residence time of the mid-estuary from 5 to 17 days. The significant decrease in discharge
coincided with a significantly higher, up to double, internal DIC load in the mid to lower estuary
(Table S9–S10). This is unexpected, and indicates that low discharge in the Elbe River in May
495 allows for a longer remineralization period of POC into DIC occurring in the mid–lower Elbe
Estuary. We deduce that this was most likely enhanced by the sufficient POC loading,
specifically to the mid-region, coupled with increased water residence time in the mid–lower
estuary regions.

500 In contrast to late spring, the summer internal DIC load in the mid and lower estuary was
significantly lower, by 35–42%, during the recent drought period between 2014 to 2020 (June–
July), compared to the non-drought period (Table S9–S10), where floods were excluded to
allow comparisons between the non-extreme situation and the drought event. For the last 3



505 years of the recent drought (2018–2020), we observed a shift in the ecosystem parameters, with
a decrease in pH down to 7.7 and an increase to positive AOU, indicating a shift to dominating
heterotrophy (Fig. 2). Findings of Kamjunke et al. (2022) confirm the efficient decomposition
of algal organic carbon in the upper Elbe Estuary (585 Elbe-km, z1) during the drought in
September 2019. Schulz et al. (in prep) reported nitrate depletion, down to 0.2 μM in this region
(585 Elbe-km), indicating nutrient limitation of primary production in late July and August
510 2018–2019. Furthermore, the FGG Elbe observed the oxygen depleted zone extended to the
upper estuary and further upstream in 2018 (Gregor Ollesch pers. Comm.). This opposes the
long-term trend of the upper estuary (z1) with dominating autotrophy in late spring and summer,
also shown in Amann et al. (2015). An extended drought period over several years, like the one
observed in the Elbe Estuary, could result in an eventual shift in carbon processing, with POC
515 decomposition and DIC production further upstream during summer, which can contribute to a
decreasing internal DIC load in the mid-lower estuary. The DIC produced as CO_2 may not be
buffered by the carbonate system in the upper estuary due to the absence of seawater containing
 CO_3^{2-} influence. Leading to CO_2 release to the atmosphere and abate along-estuary DIC export.
This suggests a prolonged impact of droughts on ecosystem functioning, and a non-linear
520 response of the ecosystem to forcing due to climate change. The potential changes in the
magnitude of CO_2 evasion in the upper estuary during the summer drought period should be
further investigated.

4.2 Controls on inorganic carbon in the lower-outer estuary

525 We find that POC loading from the upper estuary cannot account for the internal DIC load in
the lower estuary, due to a significant surplus of internal DIC load compared to POC load in
the upper estuary (Table S13), by an average of 1.3–1.9 times (Table S12). In the outer estuary,
negative AOU and higher pH indicated net autotrophy in late spring and summer. This coupled
530 with elevated POC, reaching 16% of SPM (Fig. S5), highlights increased availability of labile
OM. Higher TA compared to DIC in the outer estuary, coupled with lower $p\text{CO}_2$ to levels closer
to the respective annual mean atmospheric partial pressure (Fig. 3), corroborate the idea of net
autotrophy in the outer estuary, e.g. as described in Brasse et al. (2002). The significant positive
correlation between DIC and AOU, and negative correlation with pH, in summer in the outer
535 estuary indicate the prevalent DIC drawdown in the outer estuary, with such correlations also
found by Reimer et al. (1999) in the German Bight. However, rapid *in situ* remineralization of
the autochthonous organic carbon from the coastal region, rather than POC from the upper



estuary, could counteract a strong DIC depletion as observed in the upper estuary. For example, Reimer et al. (1999) reported up to 75% of phytoplankton was remineralized in the German
540 Bight. This newly produced OM may also be transported into the lower estuary during flood tide, and undergo remineralization subsequently producing DIC, as proposed by Voynova et al. (2015) for the area between the Delaware Bay and Murderkill Estuary.

Besides internal production of DIC, Hoppema (1993) and Voynova et al. (2019) conclude that
545 remineralization of OM within Wadden Sea sediments and subsequent DIC release into the water column considerably contribute to elevated DIC concentrations in adjacent coastal regions. The Wadden Sea coastal region, adjacent to the outer Elbe Estuary, receives around 100 g C m⁻² yr⁻¹ OM from the North Sea (van Beusekom et al., 1999). Voynova et al. (2019) also found largest TA generation in summer and autumn at 7.8-8°E, west of the outer estuary
550 (8.3-8.5°E, Fig. 1a), reaching 2400 μmol kg⁻¹ in summer 2017, exceeding summer DIC (2250 ± 50 μmol kg⁻¹) while similar to summer TA (2491 ± 71 μmol kg⁻¹) in the outer estuary. Therefore, the remineralization of OM in Wadden Sea tidal flats exported to the coastal region and facilitated by tidal flow could contribute to the enhanced DIC in the outer estuary, especially during the peak DIC in summer.

555 Freshwater and salt marshes are also adjacent to the inner and outer Elbe Estuary and are known to contribute to the estuary DIC budget (Weiss, 2013). Weiss (2013) estimated the DIC export from the tidal marshes can account for 2.8–10.2% of the mean annual DIC from the Elbe Estuary at 63.5 ± 1.4 Gmol yr⁻¹ (Amann et al., 2015). The total internal DIC load of 6.4 Gmol
560 C month⁻¹ for May to August between 1997 and 2020 (Table S12) represents 7–20% of the annual DIC export to coastal waters (Fig. 5). This highlights the importance of accounting for different carbon sources to disentangle the mechanisms responsible for carbon turnover in this region and to help improve regional and global carbon budget calculations.

565 **4.3 Tentative inorganic carbon export estimates**

The inorganic carbon in estuaries eventually settles in sediments, is released to the atmosphere as CO₂ or exported to the adjacent coastal waters (Kempe, 1982). Amann et al. (2015) deduced that the latter two were the major export pathways in the Elbe Estuary. We have estimated the
570 annual DIC air-water fluxes and lateral flux during the recovery state (Rewrie et al. in review), using the sum of the two as the estimated total export of DIC out of the Elbe Estuary.



Of the total Elbe Estuary DIC export, between 77 and 94 %, reaching $89 \pm 4.8 \text{ Gmol C yr}^{-1}$, was laterally transported to coastal waters, and thus up to 23 % was released via CO_2 evasion
575 at $10 \text{ Gmol C yr}^{-1}$, which matches the ratio between DIC export to the atmosphere and to the coastal area quantified by Amann et al. (2015). Also, the air-water CO_2 flux range (Fig. 5) places the Elbe Estuary within flux estimates for North Sea tidal estuaries (Volta et al. 2016). Amann et al. (2015) suggested the water residence time, not only influenced the CO_2 flux to the atmosphere, but also the magnitude of DIC exported to the adjacent coastal waters. Based on
580 the long-term mean annual Elbe River discharge (Fig. 2a), the Elbe Estuary was characterized by an average residence time of around 3 weeks estimated by Bergemann et al. (1996) as shown in Table S16. Whereas, the Satilla River estuary in the US was characterized by a longer average residence time of 8 weeks, and Cai and Wang (1998) calculated that 90 % of the total DIC export was CO_2 evasion to the atmosphere. In contrast, only of 4.6 % of the DIC export from
585 the Changjiang River estuary in East China was released to the atmosphere, which features a shorter residence times of a week or less (Zhai et al. 2007). This confirms the carbon cycling in estuarine and coastal waters is highly dependent on hydrological conditions.

The lowest DIC export to coastal waters of $38 \pm 5.4 \text{ Gmol}$ occurred in the drought period (2014–
590 2020), and was a 24% decrease compared to the non-drought period and excluding flood events. Severe drought conditions have previously resulted in smaller carbon exportation from estuaries to the ocean (Tian et al., 2015; Cavalcante et al., 2021). For instance, in the Mississippi River basin, all C fluxes (DIC, DOC and POC) decreased by 38% to lowest fluxes in the 2006 dry year relative to a 10 year average (Tian et al., 2015). Major changes in the river discharge, such
595 as significant reduction during prolonged drought, are therefore likely to have an impact on inorganic carbon delivery to the coastal ocean.

5 Conclusion

600 To assess the impact on the estuarine ecosystem, we compare the processes over the period of 1997 to 2020, described as the recovery state by Rewrie et al. (in review). It followed major shifts in ecosystem state after the 1980s heavy pollution. The significant increase in DIC in the mid Elbe Estuary of $6\text{--}21 \mu\text{mol kg}^{-1} \text{ yr}^{-1}$ from 1997 until 2020, during late spring and summer, is associated with a concomitant significant increase in POC, at $8\text{--}14 \mu\text{mol kg}^{-1} \text{ yr}^{-1}$, in the upper
605 estuary. The observed POC increase in the upstream waters was related to an overall



improvement in water quality, with a significant decrease in BOD₇ by over half since 1997. The significant positive correlation between the along-estuary DIC gain in the mid-estuary and POC in the upper estuary (1997–2020) indicates that the amount of POC from the upper estuary is sufficient to drive the long-term DIC increase in the mid-estuary. The decomposition of POC
610 by the mid-estuary region, prior to export to adjacent coastal waters also shows that the estuary is an efficient filter for upper estuary POC inputs.

A notable environmental driver in modulating carbon cycling in the estuary is a multi-year drought between 2014 and 2020, with significantly lower mean Elbe River discharge at $468 \pm$
615 $234 \text{ m}^3 \text{ s}^{-1}$. We find that the drought extended the dry season into late spring, lengthening the water residence time by approximately 3 times. The increased residence time allowed for a longer remineralization period for POC in May, resulting in more than doubling the internal DIC load in the mid-lower estuary, compared to the non-drought period (1997–2013). Coupled with the high POC loading from the upper estuary, this resulted in the highest internal DIC load
620 in the mid region.

In the lower to outer estuary, we find that different mechanisms likely support the maximum DIC concentrations observed here. The internal DIC load in the lower estuary was on average 1.3–1.9 times higher than the POC load from the upper estuary. We therefore postulate that
625 allochthonous from the coastal regions or autochthonous (i.e. phytoplankton) labile OM was transported into the lower estuary and remineralized there, supporting higher DIC concentrations. Additionally, the export of OM from the surrounding Wadden Sea sediments followed by remineralization within the coastal waters (Voynova et al., 2019) and import of DIC from adjacent tidal marshes (Weiss, 2013) are mechanisms that could explain high outer
630 estuary DIC concentrations. To accurately quantify DIC production, and determine the magnitude and direction of DIC loads in the lower and outer estuary, a study should concentrate on nearshore waters, whereby both flood and ebb tide must be considered.

On an annual basis, the Elbe Estuary acts as a source for CO₂, with up to $10 \text{ Gmol C yr}^{-1}$ released
635 to the atmosphere and a maximum of $89 \pm 4.8 \text{ Gmol C yr}^{-1}$ exported to adjacent coastal waters. The ratio between DIC export to the atmosphere and to the coastal area varied between 1997 and 2020, with 77–94% laterally transported to coastal waters, and only up to 23% released to the atmosphere, making the estuary an efficient system to fix carbon as DIC in outflow to the coastal regions. The DIC export to coastal waters decreased significantly in the drought period



640 to $38 \pm 5.4 \text{ Gmol C yr}^{-1}$, by 24% relative to the non-drought period average, and this shows the major effects of river discharge on the timing and magnitude of inorganic carbon export. The DIC production in and export from the Elbe Estuary is, therefore, an important factor in North Sea carbon budgets. While we have only provided tentative estimates of the changes in carbon export, we show it is essential to take into account seasonal, but also long-term changes in the
645 DIC production and consumption within an estuary to understand long-term changes in air-water CO_2 flux, DIC export to coastal waters, as well the impacts of prolonged droughts on the coastal carbonate system. This knowledge is essential for predicting carbon cycling at the land to ocean continuum.

650 *Data availability.* The data for DIC, POC and the ecosystem parameters are freely available from the data portal of the Flussgebietsgemeinschaft Elbe (FGG, River Basin Community; <https://www.fgg-elbe.de/elbe-datenportal.html>). The daily mean ambient air pressure and wind speed data are available from E-OBS meteorological data for Europe from the Copernicus Climate Data Store; <https://cds.climate.copernicus.eu>. The atmospheric CO_2 data are available
655 from the Global Monitoring Laboratory; https://gml.noaa.gov/ccgg/trends/gl_data.html.

Author contributions. LR and YV designed the concept of the study, with contributions from BB. LR conducted the data analysis and evaluation, with support by YV. LR led the writing with contributions from YV. BB, JB, AK and GO contributed to scientific input and revisions
660 of the manuscript. All authors approved the final submitted manuscript.

Competing interests. The authors declare that they have no conflict of interest

Acknowledgements. This research was funded by the CARBOSTORE" project funded by the German Federal Ministry of Education and Research, BMBF, the EU project DANUBIUS-IP (Grant agreement 101079778) and the Helmholtz Association funding program 'Changing Earth'. We thank Ulrich Wiegel for providing information on the carbon measurement methods at FGG Elbe. We are grateful to the researchers and staff at FGG Elbe for the collection of DIC and ecosystem samples. We thank Kirstin Dähnke and Gesa Schulz for providing detailed
670 information on the nitrogen cycling in the upper estuary and helpful discussions. Thanks to Vlad Macovei for providing information on using Ocean Data View.

Financial support. This work was supported by the CARBOSTORE" project funded by the German Federal Ministry of Education and Research, BMBF, the EU project DANUBIUS-IP (Grant agreement 101079778) and the Helmholtz Association funding program 'Changing Earth'.
675

References

- 680 Abril, G., Nogueira, M., Etcheber, H., Cabeçadas, G., Lemaire, E., & Brogueira, M. J.: Behaviour of organic carbon in nine contrasting European estuaries. *Estuarine, coastal and shelf science*, 54(2), 241-262, <https://doi.org/10.1006/ecss.2001.0844>, 2002.
- 685 Alfieri, L., Burek, P., Feyen, L., & Forzieri, G.: Global warming increases the frequency of river floods in Europe. *Hydrology and Earth System Sciences*, 19(5), 2247-2260, <https://doi.org/10.5194/hess-19-2247-2015>, 2015.



- 690 Amann, T., Weiss, A., & Hartmann, J.: Carbon dynamics in the freshwater part of the Elbe estuary, Germany: Implications of improving water quality. *Estuarine, Coastal and Shelf Science*, 107, 112-121, <https://doi.org/10.1016/j.ecss.2012.05.012>, 2012.
- Amann, T., Weiss, A., & Hartmann, J.: Inorganic carbon fluxes in the inner Elbe estuary, Germany. *Estuaries and Coasts*, 38, 192-210, <https://doi.org/10.1007/s12237-014-9785-6>, 2015
- 695 Apple, J. K., Del Giorgio, P. A., & Kemp, W. M.: Temperature regulation of bacterial production, respiration, and growth efficiency in a temperate salt-marsh estuary. *Aquatic Microbial Ecology*, 43(3), 243-254, doi:10.3354/ame043243, 2006.
- ARGE Elbe.: Stoffkonzentrationen in mittels Hubschrauber entnommenen Elbewasserproben (1979–1998). Arbeitsgemeinschaft zur Reinhaltung der Elbe (Report), 2000.
- 700 Barbosa P., Masante D., Arias Muñoz C., Cammalleri C., De Jager, A., Magni D., Mazzeschi M., McCormick N., Naumann G., Spinoni, J., Vogt, J.: Droughts in Europe and Worldwide 2019-2020, EUR 30719 EN, Publications Office of the European Union, Luxembourg, ISBN 978-92-76-38040-5, doi:10.2760/415204 , JRC125320, 2021.
- 705 Böhnisch, A., Mittermeier, M., Leduc, M., & Ludwig, R.: Hot spots and climate trends of meteorological droughts in Europe—assessing the percent of normal index in a single-model initial-condition large ensemble. *Frontiers in Water*, 3, 716621, <https://doi.org/10.3389/frwa.2021.716621>, 2021.
- 710 Bergemann, M., Blöcker, G., Harms, H., Kerner, M., Meyer-Nehls, R., Petersen, W., & Schroeder, F.: Der Sauerstoffhaushalt der Tideelbe. Die Küste. In: Die Küste 58. Heide, Holstein: Boyens. S. 199-261. 1996.
- Brasse, S., Nellen, M., Seifert, R., & Michaelis, W.: The carbon dioxide system in the Elbe estuary. *Biogeochemistry*, 59, 25-40, <https://doi.org/10.1023/A:1015591717351>, 2002.
- 715 Bukaveckas, P. A.: Carbon dynamics at the river–estuarine transition: a comparison among tributaries of Chesapeake Bay. *Biogeosciences*, 19(17), 4209-4226, <https://doi.org/10.5194/bg-19-4209-2022>, 2022.
- Cai, W. J.: Estuarine and coastal ocean carbon paradox: CO₂ sinks or sites of terrestrial carbon incineration?. *Annual review of marine science*, 3, 123-145, <https://doi.org/10.1146/annurev-marine-120709-142723>, 2011.
- 720 Cai, W. J., & Wang, Y.: The chemistry, fluxes, and sources of carbon dioxide in the estuarine waters of the Satilla and Altamaha Rivers, Georgia. *Limnology and Oceanography*, 43(4), 657-668, <https://doi.org/10.4319/lo.1998.43.4.0657>, 1998.
- 725 Cavalcante, M. S., Marins, R. V., da Silva Dias, F. J., & de Rezende, C. E.: Assessment of carbon fluxes to coastal area during persistent drought conditions. *Regional Studies in Marine Science*, 47, 101934, <https://doi.org/10.1016/j.rsma.2021.101934>, 2021.
- 730 Christensen, J. H., & Christensen, O. B.: Severe summertime flooding in Europe. *Nature*, 421(6925), 805-806, <https://doi.org/10.1038/421805a>, 2003.
- 735 Cornes, R., van der Schrier, G., van den Besselaar, E.J.M., Jones, P.: An Ensemble Version of the E-OBS Temperature and Precipitation Datasets, *J. Geophys. Res. Atmos.*, 123, <https://doi.org/10.1029/2017JD028200>, 2018.
- Crump, B. C., Fine, L. M., Fortunato, C. S., Herfort, L., Needoba, J. A., Murdock, S., & Prah, F. G.: Quantity and quality of particulate organic matter controls bacterial production in the Columbia River estuary. *Limnology and Oceanography*, 62(6), 2713-2731, <https://doi.org/10.1002/lno.10601>, 2017.
- 740 Dähnke, K., Sanders, T., Voynova, Y., & Wankel, S. D.: Nitrogen isotopes reveal a particulate-matter driven biogeochemical reactor in a temperate estuary. *Biogeosciences Discussions*, 1-18, <https://doi.org/10.5194/bg-19-5879-2022>, 2022.
- 745 Dickson, A. G., Sabine, C. L., & Christian, J. R.: Guide to best practices for ocean CO₂ measurements. North Pacific Marine Science Organization. <http://dx.doi.org/10.25607/OBP-1342>, 2007.



- Forzieri, G., Feyen, L., Rojas, R., Flörke, M., Wimmer, F., & Bianchi, A.: Ensemble projections of future streamflow droughts in Europe. *Hydrology and Earth System Sciences*, 18(1), 85-108, <https://doi.org/10.5194/hess-18-85-2014>, 2014.
- 750
- Geerts, L., Wolfstein, K., Jacobs, S., van Damme, S., & Vandenbruwaene, W.: Zonation of the TIDE estuaries. *Tide Report* (http://www.tide-toolbox.eu/pdf/reports/Zonation_of_the_TIDE_estuaries.pdf). 2012
- 755
- Goosen, N. K., Kromkamp, J., Peene, J., van Rijswijk, P., & van Breugel, P.: Bacterial and phytoplankton production in the maximum turbidity zone of three European estuaries: the Elbe, Westerschelde and Gironde. *Journal of Marine Systems*, 22(2-3), 151-171. [https://doi.org/10.1016/S0924-7963\(99\)00038-X](https://doi.org/10.1016/S0924-7963(99)00038-X), 1999.
- 760
- Guo, X., Cai, W. J., Zhai, W., Dai, M., Wang, Y., & Chen, B.: Seasonal variations in the inorganic carbon system in the Pearl River (Zhujiang) estuary. *Continental Shelf Research*, 28(12), 1424-143, <https://doi.org/10.1016/j.csr.2007.07.011>, 2008.
- 765
- Hardenbicker, P., Weitere, M., Ritz, S., Schöll, F., & Fischer, H.: Longitudinal plankton dynamics in the rivers Rhine and Elbe. *River Research and Applications*, 32(6), 1264-1278, <https://doi.org/10.1002/rra.2977>, 2016.
- 770
- Harding, L. W., Mallonee, M. E., Perry, E. S., Miller, W. D., Adolf, J. E., Gallegos, C. L., & Paerl, H. W.: Long-term trends, current status, and transitions of water quality in Chesapeake Bay. *Scientific Reports*, 9(1), 1-19, <https://doi.org/10.1038/s41598-019-43036-6>, 2019.
- 775
- Hitchcock, J. N., & Mitrovic, S. M.: Highs and lows: The effect of differently sized freshwater inflows on estuarine carbon, nitrogen, phosphorus, bacteria and chlorophyll a dynamics. *Estuarine, Coastal and Shelf Science*, 156, 71-82, <https://doi.org/10.1016/j.ecss.2014.12.002>, 2015.
- 780
- Hoch, M. P., & Kirchman, D. L.: Seasonal and inter-annual variability in bacterial production and biomass in a temperate estuary. *Marine ecology progress series. Oldendorf*, 98(3), 283-295, DOI: 10.3354/meps098283, 1993.
- 785
- Hoppema, J. M. J.: Carbon dioxide and oxygen disequilibrium in a tidal basin (Dutch Wadden Sea). *Netherlands journal of sea research*, 31(3), 221-229, [https://doi.org/10.1016/0077-7579\(93\)90023-L](https://doi.org/10.1016/0077-7579(93)90023-L), 1993.
- 790
- IKSE.: Die Elbe ist wieder ein lebendiger Fluss: Abschlussbericht Aktionsprogramm Elbe 1996–2010, available at: www.ikse-mkol.org/fileadmin/media/user_upload/D/06_Publikationen/03_Aktionsprogramme%20und%20Bestandsaufnahmen/2010_IKSE-APAbschlussbericht.pdf, 2010.
- 795
- IKSE.: Strategie zur Minderung der Nährstoffeinträge in Gewässer in der internationalen Flussgebietseinheit Elbe, available at: www.ikse-mkol.org/fileadmin/media/user_upload/D/06_Publikationen/01_Wasserrahmenrichtlinie/2018_IKSE_Strategie_NP.pdf, 2018.
- 800
- IPCC. : Climate Change 2022: Impacts, Adaptation and Vulnerability. Contribution of Working Group II to the Sixth Assessment Report of the Intergovernmental Panel on Climate Change [H.-O. Pörtner, D.C. Roberts, M. Tignor, E.S. Poloczanska, K. Mintenbeck, A. Alegría, M. Craig, S. Langsdorf, S. Löschke, V. Möller, A. Okem, B. Rama (eds.)]. Cambridge University Press. Cambridge University Press, Cambridge, UK and New York, NY, USA, 3056 pp., doi:10.1017/9781009325844. 2022
- 805
- Kamjunke, N., Rode, M., Baborowski, M., Kunz, J. V., Zehner, J., Borchardt, D., & Weitere, M.: High irradiation and low discharge promote the dominant role of phytoplankton in riverine nutrient dynamics. *Limnology and Oceanography*, 66(7), 2648-2660, <https://doi.org/10.1002/lno.11778>, 2021.
- 810
- Kamjunke, N., Beckers, L. M., Herzsprung, P., von Tümpling, W., Lechtenfeld, O., Tittel, J., Risse-Buhl, U., Rode, M., Wachholz, A., Kallies, R. and Schulze, T., Krauss, M., Brack, W., Comero, S., Gawlik, B. M., Skejo, H., Tavazzi, S., Mariani, G., Borchardt, D., & Weitere, M.: Lagrangian profiles of riverine autotrophy, organic matter transformation, and micropollutants at extreme drought. *Science of The Total Environment*, 828, 154243, <https://doi.org/10.1016/j.scitotenv.2022.154243>, 2022.
- 815
- Kaushal, S. S., Likens, G. E., Utz, R. M., Pace, M. L., Grese, M., & Yepsen, M.: Increased river alkalinization in the Eastern US. *Environmental science & technology*, 47(18), 10302-10311, <https://doi.org/10.1021/es401046s>, 2013.



- 810 Kempe, S.: Valdivia cruise, October 1981: carbonate equilibria in the estuaries of Elbe, Weser, Ems and in the Southern German Bight. *Transport of Carbon and Minerals in Major World Rivers*, 1, 719-742, 1982.
- Kienzler, S., Pech, I., Kreibich, H., Müller, M., & Thieken, A. H.: After the extreme flood in 2002: changes in preparedness, response and recovery of flood-affected residents in Germany between 2005 and 2011. *Natural Hazards and Earth System Sciences*, 15(3), 505-526, <https://doi.org/10.5194/nhess-15-505-2015>, 2015.
- 815 Langhammer, J.: Water quality changes in the Elbe River basin, Czech Republic, in the context of the post-socialist economic transition. *GeoJournal*, 75(2), 185-198, <https://doi.org/10.1007/s10708-009-9292-7>, 2010.
- Lan, X., Tans, P. and K.W. Thoning: Trends in globally-averaged CO₂ determined from NOAA Global Monitoring Laboratory measurements. Version 2023-03 NOAA/GML, available at: https://gml.noaa.gov/ccgg/trends/gl_data.html, last access: 16 March 2023.
- 820 Lewis, E., and Wallace, D.: Program developed for CO₂ system calculations, Environmental System Science Data Infrastructure for a Virtual Ecosystem, 1998.
- 825 Moravec, V., Markonis, Y., Rakovec, O., Svoboda, M., Trnka, M., Kumar, R., & Hanel, M.: Europe under multi-year droughts: how severe was the 2014–2018 drought period?. *Environmental Research Letters*, 16(3), 034062, DOI 10.1088/1748-9326/abe828, 2021.
- 830 Norbistrath, M., Pätsch, J., Dähnke, K., Sanders, T., Schulz, G., van Beusekom, J. E., & Thomas, H.: Metabolic alkalinity release from large port facilities (Hamburg, Germany) and impact on coastal carbon storage. *Biogeosciences*, 19(22), 5151-5165, <https://doi.org/10.5194/bg-19-5151-2022>, 2022.
- Orr, J. C., Epitalon, J. M., Dickson, A. G., & Gattuso, J. P.: Routine uncertainty propagation for the marine carbon dioxide system. *Marine Chemistry*, 207, 84-107, <https://doi.org/10.1016/j.marchem.2018.10.006>, 2018.
- 835 Raymond, P. A., Oh, N. H., Turner, R. E., & Broussard, W.: Anthropogenically enhanced fluxes of water and carbon from the Mississippi River. *Nature*, 451(7177), 449-452, <https://doi.org/10.1038/nature06505>, 2008.
- 840 Reimer, A., Brasse, S., Doerffer, R., Durselen, C.D., Kempe, S., Michaelis, W., Rick, H.J., & Siefert, R.: Carbon cycling in the German Bight: An estimate of transformation processes and transport, *German Journal of Hydrography*, 51, 313–329, DOI: 10.1007/BF02764179 1999.
- Rewrie, L.C.V.R., Voynova, Y.G., Beusekom, J.E.E., Sanders, T., Körtzinger, A., Brix, H., Ollesch, G., Baschek, B. (in review). Significant shifts in inorganic carbon and ecosystem state in a temperate estuary (1985-2018). *Limnology and Oceanography*.
- 845 Sanders, T., Schöl, A., & Dähnke, K.: Hot spots of nitrification in the Elbe estuary and their impact on nitrate regeneration. *Estuaries and coasts*, 41, 128-138, <https://doi.org/10.1007/s12237-017-0264-8>, 2018.
- 850 Sharp, J. H.: Estuarine oxygen dynamics: What can we learn about hypoxia from long-time records in the Delaware Estuary?. *Limnology and Oceanography*, 55(2), 535-548, <https://doi.org/10.4319/lo.2010.55.2.0535>, 2010.
- Schöl, A., Hein, B., Wyrwa, J., & Kirchesch, V.: Modelling water quality in the Elbe and its estuary—Large scale and long term applications with focus on the oxygen budget of the estuary. *Die Küste*, 81 Modelling, (81), 203-232, 2014.
- 855 Schulz, G., van Beusekom, J. E. E., Jacob, J., Bold, S., Schöl, A., Ankele, M., Sanders, T., and Dähnke, K.: (in prep.). Low discharge intensifies nitrogen retention in rivers – a case study in the Elbe River
- 860 Tian, H., Ren, W., Yang, J., Tao, B., Cai, W.J., Lohrenz, S.E., Hopkinson, C.S., Liu, M., Yang, Q., Lu, C. & Zhang, B.: Climate extremes dominating seasonal and interannual variations in carbon export from the Mississippi River Basin. *Global Biogeochemical Cycles*, 29(9), pp.1333-1347, <https://doi.org/10.1002/2014GB005068>, 2015.
- 865 Van Beusekom, J. E. E., Brockmann, U. H., Hesse, K. J., Hickel, W., Poremba, K., & Tillmann, U.: The importance of sediments in the transformation and turnover of nutrients and organic matter in the Wadden Sea and German Bight. *German Journal of Hydrography*, 51(2-3), 245-266, DOI: 10.1007/BF02764176, 1999.



- 870 Van Beusekom, J. E., Carstensen, J., Dolch, T., Grage, A., Hofmeister, R., Lenhart, H., Kerimoglu, O., Kolbe, K., Pätsch, J., Rick, J. and Rönn, L., & Ruiter, H.: Wadden Sea Eutrophication: long-term trends and regional differences. *Frontiers in Marine Science*, 6, 370, <https://doi.org/10.3389/fmars.2019.00370>, 2019.
- 875 Volta, C., Laruelle, G. G., & Regnier, P.: Regional carbon and CO₂ budgets of North Sea tidal estuaries. *Estuarine, Coastal and Shelf Science*, 176, 76-90, <https://doi.org/10.1016/j.ecss.2016.04.007>, 2016.
- Voynova, Y. G., Lebaron, K. C., Barnes, R. T., & Ullman, W. J.: In situ response of bay productivity to nutrient loading from a small tributary: The Delaware Bay-Murderkill Estuary tidally-coupled biogeochemical reactor. *Estuarine, Coastal and Shelf Science*, 160, 33-48, <https://doi.org/10.1016/j.ecss.2015.03.027>, 2015.
- 880 Voynova, Y. G., Brix, H., Petersen, W., Weigelt-Krenz, S., & Scharfe, M.: Extreme flood impact on estuarine and coastal biogeochemistry: the 2013 Elbe flood. *Biogeosciences*, 14(3), 541-557, <https://doi.org/10.5194/bg-14-541-2017>, 2017.
- 885 Voynova, Y. G., Petersen, W., Gehrung, M., Aßmann, S., & King, A. L.: Intertidal regions changing coastal alkalinity: The Wadden Sea-North Sea tidally coupled bioreactor. *Limnology and Oceanography*, 64(3), 1135-1149, <https://doi.org/10.1002/lno.11103>, 2019.
- 890 Watts, G., Battarbee, R. W., Bloomfield, J. P., Crossman, J., Daccache, A., Durance, I., ... & Wilby, R. L.: Climate change and water in the UK—past changes and future prospects. *Progress in Physical Geography*, 39(1), 6-28, <https://doi.org/10.1177/0309133314542957>, 2015.
- Wanninkhof, R.: Relationship between wind speed and gas exchange over the ocean revisited. *Limnology and Oceanography: Methods*, 12(6), 351-362, <https://doi.org/10.4319/lom.2014.12.351>, 2014.
- 895 Weiss, R.: Carbon dioxide in water and seawater: the solubility of a non-ideal gas. *Marine chemistry*, 2(3), 203-215, [https://doi.org/10.1016/0304-4203\(74\)90015-2](https://doi.org/10.1016/0304-4203(74)90015-2), 1974.
- Weiss, R. F., & Price, B. A.: Nitrous oxide solubility in water and seawater. *Marine chemistry*, 8(4), 347-359, [https://doi.org/10.1016/0304-4203\(80\)90024-9](https://doi.org/10.1016/0304-4203(80)90024-9), 1980.
- 900 Weiss, A.: The silica and inorganic carbon system in tidal marshes of the Elbe estuary, Germany: fluxes and spatio-temporal patterns (Thesis). Staats- und Universitätsbibliothek Hamburg Hamburg. 2013.
- 905 Williams, A. P., Seager, R., Abatzoglou, J. T., Cook, B. I., Smerdon, J. E., & Cook, E. R.: Contribution of anthropogenic warming to California drought during 2012–2014. *Geophysical Research Letters*, 42(16), 6819-6828, <https://doi.org/10.1002/2015GL064924>, 2015.
- 910 Zhai, W., Dai, M., & Guo, X.: Carbonate system and CO₂ degassing fluxes in the inner estuary of Changjiang (Yangtze) River, China. *Marine chemistry*, 107(3), 342-356, <https://doi.org/10.1016/j.marchem.2007.02.011>, 2007.
- Zink, M., Samaniego, L., Kumar, R., Thober, S., Mai, J., Schäfer, D., & Marx, A.: The German drought monitor. *Environmental Research Letters*, 11(7), 074002, DOI 10.1088/1748-9326/11/7/074002, 2016.